PCCP

Accepted Manuscript

ROYAL SOCIETY OF CHEMISTRY

www.rsc.org/pccp

A Combined Crossed Molecular Beams and ab Initio Investigation on the Formation of Vinylsulfidoboron ($C_2H_3{}^{11}B^{32}S$)

Tao Yang, Beni B. Dangi, Dorian S. N. Parker, Ralf I. Kaiser*

Department of Chemistry, University of Hawaii at Manoa, Honolulu, Hawaii 96822, USA

Yi An, Agnes H. H. Chang

Department of Chemistry, National Dong Hwa University, Shoufeng, Hualien 974, Taiwan

* Corresponding Author:

Professor Dr. Ralf I. Kaiser; E-mail: ralfk@hawaii.edu; Phone: 808-956-5731

Abstract

We exploited crossed molecular beams techniques and electronic structure calculations to provide compelling evidence that the vinylsulfidoboron molecule ($C_2H_3{}^{11}B^{32}S$) – the simplest member of hitherto elusive olefinic organo-sulfidoboron molecules (RBS) – can be formed via the gas phase reaction of boron monosulfide ($^{11}B^{32}S$) with ethylene (C_2H_4) under single collision conditions. The reaction mechanism follows indirect scattering dynamics via a barrierless addition of the boron monosulfide radical to the carbon-carbon double bond of ethylene. The initial reaction complex can either decompose to vinylsulfidoboron ($C_2H_3{}^{11}B^{32}S$) via the emission of a hydrogen atom from the sp^3 hybridized carbon atom, or isomerize via a 1,2-hydrogen shift prior to a hydrogen loss from the terminal carbon atom to form vinylsulfidoboron. Statistical (RRKM) calculations predict branching ratios of 8 % and 92 % for both pathways leading to vinylsulfidoboron, respectively. A comparison between the boron monosulfide ($^{11}B^{32}S$) plus ethylene and the boron monoxide (^{11}BO) plus ethylene systems indicate that both reactions follow similar reaction mechanisms involving addition – elimination and addition – hydrogen migration – elimination pathways. Our experimental findings open up a novel pathway to access the previously poorly-characterized class of organo-sulfidoboron molecules via bimolecular gas phase reactions, which are difficult to form through ‘classical’ organic synthesis.

1. Introduction

During recent years, boron-based fuels have received considerable attention due to their enhanced gravimetric and volumetric energy density compared to traditional carbon-based fuels such as JP-8.[1-6] The key obstacle that exists for practical combustion processes involving boron-based fuels is the formation of a protective layer of boron oxide (B_2O_3), which prohibits the actual ignition of boron particles. Therefore, extensive theoretical and experimental efforts have been conducted to fully characterize the complex processes of boron ignition and combustion at the molecular level.[2, 7-10] When boron is employed as millimeter- to centimeter-sized pellets serving as an additive to conventional hydrocarbon-based fuels, the hydrocarbon-based fuels ignite to reach a temperature high enough to remove the boron oxide (B_2O_3) layer, which in turn makes boron accessible for the combustion processes.[7, 9, 11] Thus, an understanding of boron-based combustion processes requires a detailed knowledge of the underlying elementary reactions between boron-bearing transient reactants and hydrocarbon molecules. Consequently, the reaction dynamics of atomic boron in its electronic ground state (^2P) with unsaturated hydrocarbons such as acetylene (C_2H_2),[12-13] ethylene (C_2H_4),[14-15] benzene (C_6H_6),[16-17] allene (CH_2CCH_2),[18] methylacetylene (CH_3CCH),[19] diacetylene (HCCCCH),[20] and dimethylacetylene (CH_3CCCH_3)[21] have been studied under single collision conditions utilizing the crossed molecular beams approach. These studies led to the identification of hitherto elusive organoboron molecules of relevance to boron-based combustion systems (Figure 1).[22]

The oxidation of boron itself involves multiple steps, which can be presented schematically by the reaction sequence $B \rightarrow BO \rightarrow BO_2 \rightarrow B_2O_3$.[23] Therefore, the boron monoxide radical (BO) is expected to play a crucial role in coupling the boron-oxygen with the hydrocarbon chemistries.

The flash vacuum pyrolysis of triphenyl- and trimethylboroxin in Argon matrix and at low temperature below 20 K followed by gas phase products trapping yielded phenyl(oxo)borane (C_6H_5BO) and methyl(oxo)borane (CH_3BO), which were characterized by IR spectroscopy.[24] In recent years, our group has systematically investigated the reactions of the boron monoxide radical with unsaturated hydrocarbons such as acetylene (C_2H_2),[25] ethylene (C_2H_4),[26] methylacetylene (CH_3CCH),[27] diacetylene (HCCCCH),[28] dimethylacetylene (CH_3CCCH_3),[29] as well as benzene (C_6H_6)[30] under single collision conditions utilizing a crossed molecular beams machine. These bimolecular gas phase reactions led to the identification of previously unknown organoboronyl molecules formed via de-facto barrierless addition of the boron monoxide radical to the π-electron density of the unsaturated hydrocarbons via indirect scattering dynamics, followed by atomic hydrogen and/or methyl group loss in overall exoergic reactions (Figure 2).

Although the reaction dynamics of the boron monoxide radical with unsaturated hydrocarbons have been studied systematically under single collision conditions and a general trend on the reactivity and reaction mechanism has emerged (barrierless addition, indirect complex forming reaction, atomic hydrogen and/or methyl group elimination, tight exit transition states), *neither theoretical nor experimental studies exist on the reaction dynamics of the isovalent boron monosulfide radical ($^{11}B^{32}S$; $X^2\Sigma^+$) with unsaturated hydrocarbons*. These reactions are expected to lead to the synthesis of hitherto poorly-studied organo-sulfidoboron compounds (RBS). As isovalent radicals, boron monosulfide and boron monoxide share some similarities and discrepancies. Both radicals have nine valence electrons and their ground electronic states are identical: $X^2\Sigma^+$.[31] The bond dissociation energies of boron monosulfide and boron monoxide have been determined to be 5.82 eV [32] and 8.28 eV, respectively.[33] This discrepancy is also

reflected in the longer B-S bond of about 161 pm,[31-32, 34] while the B-O bond length is only about 120 pm.[31]

Traditional syntheses of sulfidoborons date back to 1967. Here, the reaction of hydrogen sulfide (H_2S) vapor with crystalline boron in a quartz tube at a temperature of around 1,500 K resulted in the formation of the stem compound thioborine (HBS).[35-37] The first and only organo-sulfidoboron characterized to date – methylsufidoboron (CH_3BS) was synthesized via the reaction of crystalline boron with dimethyl disulfide (CH_3SSCH_3) at around 1,200 K in a quartz tube.[38] Compared with the B-S bond distance of 159.78 pm in thioborine,[39-40] the B-S bond in methylsufidoboron was probe to be 160.22 pm, which indicates the tendency of bond extension upon substituting a hydrogen atom by a methyl group.[41] However, the short-lived methylsufidoboron and its tendency to trimerize limited traditional synthetic pathways to organo-sulfidoboron molecules. Here, we propose a versatile approach to synthesize monomers of organo-sulfidoboron molecules in the gas phase under single collision conditions using the crossed molecular beams apparatus.[42-44] The single collision encounter of boron monosulfide radical (BS) in its $^2\Sigma^+$ electronic ground state with ethylene (C_2H_4; X^1A_g) followed by indirect reaction dynamics completely reduces trimerization of the monomer, i.e. the nascent reaction product. Therefore, this technique represents a powerful experimental method to conduct chemical reactions in the gas phase and to observe the outcome for the reaction of a single boron monosulfide radical with only one ethylene molecule forming highly reactive molecules, which are difficult to synthesize via 'classical' organic chemistry.

(1) $$C_2H_4 + BS \rightarrow C_2H_3BS + H$$

2. Methods

2.1 Experimental and Data Analysis

The gas phase reaction between the boron monosulfide radical (BS; $X^2\Sigma^+$) and ethylene (C_2H_4; X^1A_g) was conducted at the molecular level under single collision conditions exploiting a crossed molecular beams machine.[42-44] A pulsed supersonic beam of boron monosulfide radicals was generated *in situ* by laser ablation of a boron rod at 266 nm[45] and subsequently entraining the ablated boron atoms into carbon disulfide (CS_2; 99.9%) seeded in helium gas (He; 99.9999%; 1.8 atm). The boron monosulfide radical beam was collimated and velocity selected (peak velocity v_p = 1162 ± 15 ms^{-1}; speed ratio S = 5.1 ± 0.2) by a four-slot chopper wheel, and then perpendicularly intersected a supersonic beam of pure ethylene gas (C_2H_4; 99.999 %) with a peak velocity of v_p = 883 ± 15 ms^{-1} and speed ratio of S = 7.0 ± 0.3 in the scattering chamber, at a collision energy of 18 ± 1 $kJmol^{-1}$. The reaction products were monitored by a rotatable quadrupole mass spectrometer after electron impact ionization of the neutral products at 80 eV in an ultra-high vacuum chamber held at about 2 × 10^{-12} torr. The velocity distributions of the products were collected through the angular-resolved time-of-flight (TOF) technique, that is, recording the arrival time of ions at well-defined mass-to-charge ratios (*m/z*) of the ionized products, at different scattering angles. The TOF spectra and the LAB angular distribution were fit with Legendre polynomials using a forward-convolution routine, which utilizes an initially-parameterized functions of the product translational energy flux distribution $P(E_T)$ and angular flux distribution $T(\theta)$ in the center-of-mass (CM) frame to iteratively optimize the TOF spectra and angular distribution in the LAB frame until the best fits are reached.[46-48] As a result, we depict the product flux contour map $I(\theta,u) = P(u) \times T(\theta)$, which represents the intensity of the reactively scattered products (I) as a function of the CM scattering angle (θ) and the product velocity (u). This plot presents the differential cross section and gives an image of the studied chemical reaction.[49]

2.2 Computational Methods

Here, the geometries of various species involved in the reaction of the boron monosulfide radical (BS; $X^2\Sigma^+$) and ethylene (C_2H_4;X^1A_g) were computed via *ab initio* electronic structure calculations. Intermediates, transition states, and dissociation products are characterized such that their optimized geometries and harmonic frequencies are obtained with the unrestricted B3LYP/cc-pVTZ,[50-51] and the energies are refined with the coupled cluster[52-55] CCSD(T)/cc-pVTZ with B3LYP/cc-pVTZ zero-point energy corrections (Table S1 & S2). Note that the optimized geometry and harmonic frequencies of tsi1p1 are computed with mp2/cc-pVTZ due to unsuccessful B3LYP/cc-pVTZ attempts. Calculations utilizing more costly basis set of aug-cc-pVTZ for B3LYP functional are also performed, and however, yield similar results in both relative energies and geometries for the present system as seen in Supporting Information (Table S3 & S4). The barrierless formation of the collision complex is confirmed by intrinsic reaction coordinate calculations (IRC) at B3LYP/cc-pVTZ level of theory along the C-B bond distance. The GAUSSIAN 03 program is utilized in the electronic structure calculations; the relative energies are expected to be accurate within ± 5 kJ mol^{-1}.[56] Rate constants *k(E)* are calculated according to RRKM theory (Table S5).[57] Product branching ratios are obtained by solving the rate equations based on the predicted reaction paths.

3. Results

The TOF spectra were accumulated accounting for the natural abundances of boron (^{11}B, ^{10}B) and sulfur (^{34}S, ^{33}S, ^{32}S) in the boron monosulfide reactant. These isotopes result in reactant masses from 45 amu ($^{11}B^{34}S$) down to 42 amu ($^{10}B^{32}S$). The TOF spectra of potential atomic and molecular hydrogen loss channels upon the reaction of boron monosulfide with ethylene (C_2H_4;

28 amu) were probed from mass-to-charge ratios, *m/z*, of 72 ($C_2H_3{}^{11}B^{34}S^+$) to *m/z* of 66 ($C_2{}^{10}B^{32}S^+$); these data were found to be superimposable after scaling. We therefore collected TOF spectra at *m/z* of 70 ($C_2H_3{}^{11}B^{32}S^+$) which depicts the best signal-to-noise ratio; the corresponding laboratory angular distribution was obtained by integrating the time-of-flight spectra and scaling for the data accumulation time (Figure 3). Both of the TOF spectra and the laboratory angular distribution were fit with a single channel involving the mass combination of 70 amu (C_2H_3BS) and 1 amu (H). Therefore, we conclude that an atomic hydrogen elimination channel for the reaction of boron monosulfide with ethylene is open and that a product of the molecular formula $C_2H_3{}^{11}B^{32}S$ (hereafter: C_2H_3BS; 70 amu) is formed. In addition, the corresponding laboratory angular distribution peaks at an angle close to the center-of-mass (CM) angle of 27.1° ± 0.8° and spans a scattering range of about 40° (Figure 3). These findings propose an indirect reaction mechanism and the involvement of C_2H_4BS collision complex(es).[58]

Our goal is not only to assign the molecular formula of the reaction product(s), but also to attribute the chemical structure(s) and the underlying reaction mechanism. Hence it is crucial to extract information on the chemical dynamics from the experimental data. This is accomplished by exploiting a forward-convolution routine to transfer the laboratory data (TOF spectra, laboratory angular distribution) to the data in the CM reference frame. This approach leads to the 'best fit' functions: the CM translational energy flux distribution $P(E_T)$ and the CM angular flux distribution $T(\theta)$ (Figure 4). Based on the best fit functions, we concluded that $P(E_T)$ extends up to 62 ± 12 kJ mol^{-1} . For those products formed without internal excitation, the high-energy cutoff represents the sum of the absolute reaction energy and the collision energy; thus we determined the reaction energy to be -44 ± 13 kJ mol^{-1} for this reaction system considering our

collision energy of 18.0 ± 1.0 kJ mol^{-1}. Further, $P(E_T)$ depicts the distribution maximum of 22 ± 9 kJ mol^{-1} indicating a relatively tight exist transition state(s) upon the decomposition of C_2H_4BS complex(es) to the final product(s). For the reversed reaction, we expect to find an entrance barrier of the same order of magnitude, when the hydrogen atom reacts with the closed shell C_2H_3BS isomer(s) due to the principle of the microscopic reversibility of a chemical reaction.[58]

The center-of-mass angular flux distribution, $T(\theta)$, also delivers important information on the reaction dynamics. First, $T(\theta)$ displays intensity all over the complete angular range, which indicates an indirect reaction mechanism via bound C_2H_4BS intermediate(s).[58] Second, the intensity ratios at poles, $I(180°)/I(0°)$, was found to be 0.4 ± 0.1, and the angular distribution is slightly asymmetric with respect to 90°, which depicts an enhanced flux in the forward hemisphere with respect to the primary radial beam. This feature reflects that the decomposing intermediate can be classified as an 'osculating complex'[59] with a lifetime that is comparable to, or slightly shorter than its rotational period.[60] Lastly, we observed that the CM angular distribution depicts a peak intensity at around $\theta = 83°$ indicating that the decomposing complex preferentially emits a hydrogen atom almost parallel to the total angular momentum vector and nearly perpendicular to the rotational plane of the decomposing complex (sideways scattering).[58] These geometrical constraints have also been identified, for instance, in the reactions of isovalent cyano (CN)[61] and boron monoxide (^{11}BO)[26] radicals with ethylene.

4. Discussion

Considering the reaction exoergicity to form the C_2H_3BS isomers plus atomic hydrogen to be -44 ± 13 kJ mol^{-1}, we can compare the experimentally-determined reaction exoergicity with the energetics obtained from electronic structure computations for distinct C_2H_3BS isomers. The

computations indicate the formation of three C_2H_3BS isomers (**p1** to **p3**): vinylsulfidoboron (**p1**, C_2H_3BS), methylsulfidoboroncarbene (**p2**, CH_3CBS), and vinylisosulfidoboron (**p3**, C_2H_3SB) (Figure 5). The calculations predict that vinylsulfidoboron is more stable by 314 kJ mol^{-1} compared to the vinylisosulfidoboron isomer. Recall that the preferential stability of the sulfidoboron structure compared to the isosulfidoboron structure correlates nicely with the previous study by Mebel *et al.*,[62] indicating that HBS is thermodynamically more stable by 258 $kJmol^{-1}$ compared to the HSB isomer. Further, the theoretical calculations predict an overall reaction exoergicity of -39 ± 5 kJ mol^{-1} to form vinylsulfidoboron (C_2H_3BS) plus atomic hydrogen; this agrees very well with the experimentally-determined reaction exoergicity of -44 ± 13 kJ mol^{-1}. The carbene structure methylsulfidoboroncarbene (**p2**, CH_3CBS) and the vinylisosulfidoboron (**p3**, C_2H_3SB) isomers are energetically not accessible under single collision conditions since the computed endergonic reaction energies of 255 and 275 kJ mol^{-1} could not be compensated by the collision energy of about 18.0 ± 1.0 kJ mol^{-1}. Therefore, we can deduce that vinylsulfidoboron (C_2H_3BS) presents the sole product in the reaction of boron monosulfide with ethylene. In summary, our experiment observed for the very first time the vinylsulfidoboron molecule (C_2H_3BS).

How is the vinylsulfidoboron molecule (C_2H_3BS) formed under single collision conditions? A comparison between the molecular structures of the reactants and the product proposes that one of the four chemically equivalent hydrogen atoms in the ethylene reactant is effectively replaced by the boron monosulfide moiety. This requires the formation of a C-B bond and the cleavage of a C-H bond to yield the vinylsulfidoboron molecule (C_2H_3BS). The computations indicate that the boron monosulfide radical adds without barrier to the π electron density of the C-C double

bond of the ethylene molecule leading to intermediate **i1**, which is stabilized by 175 kJ mol^{-1} with respect to the separated reactants. Intermediate **i1** either isomerizes via hydrogen shift from the C1 to the C2 carbon atom forming **i2** over a barrier of 132 kJ mol^{-1} or undergoes unimolecular decomposition by emitting a hydrogen atom from the sp^3 hybridized carbon atom. The latter pathway leads to the formation of the vinylsulfidoboron molecule (C_2H_3BS) and involves a tight exit transition state located 21 kJ mol^{-1} above the separated products. Alternatively, **i2** can fragment by emitting atomic hydrogen from the C2 carbon atom leading to vinylsulfidoboron (C_2H_3BS); this pathway has a relatively loose exit transition state of only 8 kJ mol^{-1} above the separated products. Recall that the CM translational energy flux distribution predicted at least one channel to have an exit barrier in the order of 22 ± 9 kJ mol^{-1} upon the decomposition to the vinylsulfidoboron molecule (C_2H_3BS). Therefore, we can conclude that at least a fraction of the collision complexes **i1** undergoes unimolecular decomposition forming the vinylsulfidoboron molecule (C_2H_3BS) plus atomic hydrogen. Based on the experimental data alone, we cannot quantify the involvement of **i2** leading to vinylsulfidoboron via atomic hydrogen loss. Finally, let us have a look at the structures of the exit transition states related to the decomposition of **i1** and **i2**. Here, the hydrogen atom is predicted to be emitted at angles of about 91.1^o and 88.3^o with respect to the rotational plane of the respective decomposing complex (Figure 6). Therefore, the experimentally-predicted sideways scattering can be well matched with the existence and decomposition of intermediate(s) **i1** and/or **i2**. However, if we assume that the available energy is equilibrated among molecular degrees of freedom before the reaction occurs and considering that energy is conserved, the rate constants for the reaction steps can also be predicted by RRKM theory.[25-26] These calculations suggest that 92 % of the vinylsulfidoboron

molecule (C_2H_3BS) is formed via the unimolecular decomposition of **i2**, while only 8 % of the final product is formed via the fragmentation of **i1**.

It is attractive to compare the reaction mechanism of the boron monosulfide radical ($^{11}B^{32}S$; $X^2\Sigma^+$) plus ethylene (C_2H_4; X^1A_g) with the isoelectronic reaction between the boron monoxide radical (^{11}BO; $X^2\Sigma^+$) plus ethylene (C_2H_4; X^1A_g) studied earlier in our group.[26] Following indirect dynamics, the boron monoxide radical adds its boron atom to one carbon atom of the ethylene molecule barrierlessly. The initial reaction intermediate either decomposes to the vinyl boron monoxide ($C_2H_3{}^{11}BO$) via a hydrogen emission from the sp^3 hybridized carbon atom via a tight exit transition state, or involves a 1,2-hydrogen shift to form $CH_3CH^{11}BO$ followed by a hydrogen loss from the terminal carbon atom to vinyl boron monoxide via a relatively loose exit transition state. These features are similar to those in the reaction of boron monosulfide with ethylene, and the $CH_2CH_2{}^{11}BO$ and $CH_3CH^{11}BO$ intermediates are analogous to **i1** and **i2** in the current reaction system. In addition, the geometrical constraints upon the hydrogen emissions from the decomposing complexes $CH_2CH_2{}^{11}BO$ and $CH_3CH^{11}BO$ show preferred sideways scattering that is very similar to the case in the $^{11}B^{32}S$ plus C_2H_4 system. Lastly, the RRKM calculations for the formation of vinyl boron monoxide indicate that the branching ratios for the hydrogen loss channels from $CH_2CH_2{}^{11}BO$ and $CH_3CH^{11}BO$ contribute 44 % and 56 % to the total yield of vinyl boron monoxide, respectively. In the reaction system of boron monosulfide with ethylene to vinylsulfidoboron, the branching ratios to the final product system from the direct decomposition channel and the channel involving hydrogen migration and decomposition are 8% and 92%, respectively. Therefore, both of $^{11}B^{32}S$ plus C_2H_4 and ^{11}BO plus C_2H_4 systems actually share strong similarities on the reaction mechanism.

5. Conclusions

Exploiting the crossed molecular beams technique and electronic structure calculations, we have provided compelling evidence that the vinylsulfidoboron molecule ($C_2H_3{}^{11}B^{32}S$) – the simplest member of an olefinic organo-sulfidoboron molecule (RBS) – can be formed in the gas phase via a bimolecular reaction under single collision conditions. The route to form an organo-sulfidoboron molecule via the reaction of the boron monosulfide radical with an unsaturated hydrocarbon molecule can be considered as a prototype study to form even more complicated, hitherto elusive organosulfidoborons in the gas phase via a directed synthesis under single collision conditions. Considering the isoelectronicity of the $^{11}B^{32}S$ – C_2H_4 and ^{11}BO – C_2H_4 systems and the facile formation of $C_2H_3{}^{11}B^{32}S$ and $C_2H_3{}^{11}BO$ respectively, we can predict that hitherto elusive organo-sulfidoborons can be synthesized via bimolecular gas phase reactions of the boron monosulfide radical with unsaturated hydrocarbons (Figure 7), thus opening up a novel path to access the previously poorly-characterized class of organo-sulfidoboron molecules, which would be difficult to synthesize through 'classical' synthesis.

Supporting Information

Two tables giving calculated energies of collision complexes, intermediates, transition states, and dissociation products for the B3LYP/cc-pVTZ optimized geometries and the B3LYP/aug-cc-pVTZ optimized geometries respectively, two tables containing optimized Cartesian coordinates (Å), rotational constants (GHz) and vibrational frequencies (cm^{-1}) of reactants, intermediates, transition states, and dissociation products computed for the reaction of boron monosulfide (BS; $X^2\Sigma^+$) with ethylene (C_2H_4; X^1A_g) at the cc-pVTZ basis set and at the aug-cc-pVTZ basis set

respectively, and a table giving RRKM rate constants computed with B3LYP/cc-pVTZ frequencies and CCSD(T)/cc-pVTZ energies at various collision energies.

Acknowledgements

We acknowledge the support of this project by the Air Force Office of Scientific Research (FA9550-12-1-0213). Computer resources at the National Center for High-performance Computer of Taiwan were utilized in the calculations.

References

1. M. K. King, *J. Spacecr. Rockets*, 1982, **19**, 294-306.
2. C. L. Yeh and K. K. Kuo, *Prog. Energy Combust. Sci.*, 1996, **22**, 511-541.
3. K. K. Kuo and R. Pein, *Combustion of Boron-based Solid Propellants and Solid Fuels*, Begell House/CRC Press: Redding, Connecticut, USA, 1993.
4. J. A. Nabity, T.-H. Lee, B. Natan and D. W. Netzer, *Int. J. Energ. Mater. Chem. Propul.*, 1993, **2**, 287-302.
5. A. Gany, *Int. J. Energ. Mater. Chem. Propul.*, 1993, **2**, 91-112.
6. B. Natan and A. Gany, *J. Propul. Power*, 1991, **7**, 37-43.
7. R. A. Yetter, F. L. Dryer, H. Rabitz, R. C. Brown and C. E. Kolb *A Comprehensive Physical and Numerical Model of Boron Particle Ignition*, Symp. Int. Combust. Proc., Elsevier: 1996; 1909-1917.
8. W. Zhou, R. Yetter, F. Dryer, H. Rabitz, R. Brown and C. Kolb, *Combust. Flame*, 1999, **117**, 227-243.
9. R. Brown, C. Kolb, R. Yetter, F. Dryer and H. Rabitz, *Combust. Flame*, 1995, **101**, 221-238.
10. R. Brown, C. Kolb, H. Rabitz, S. Cho, R. Yetter and F. Dryer, *Int. J. Chem. Kinet.*, 1991, **23**, 957-970.
11. R. Brown, C. Kolb, S. Cho, R. Yetter, F. Dryer and H. Rabitz, *Int. J. Chem. Kinet.*, 1994, **26**, 319-332.
12. F. Zhang, X. Gu, R. I. Kaiser and H. Bettinger, *Chem. Phys. Lett.*, 2008, **450**, 178-185.
13. R. Kaiser, N. Balucani, N. Galland, F. Caralp, M. Rayez and Y. Hannachi, *Phys. Chem. Chem. Phys.*, 2004, **6**, 2205-2210.
14. N. Balucani, O. Asvany, Y. T. Lee, R. I. Kaiser, N. Galland and Y. Hannachi, *J. Am. Chem. Soc.*, 2000, **122**, 11234-11235.
15. F. Zhang, X. Gu, R. I. Kaiser, N. Balucani, C. H. Huang, C. H. Kao and A. H. H. Chang, *J. Phys. Chem. A*, 2008, **112**, 3837-3845.
16. F. Zhang, Y. Guo, X. Gu and R. I. Kaiser, *Chem. Phys. Lett.*, 2007, **440**, 56-63.
17. H. F. Bettinger and R. I. Kaiser, *J. Phys. Chem. A*, 2004, **108**, 4576-4586.
18. F. Zhang, H. L. Sun, A. H. H. Chang, X. Gu and R. I. Kaiser, *J. Phys. Chem. A*, 2007, **111**, 13305-13310.
19. F. Zhang, C. H. Kao, A. H. H. Chang, X. Gu, Y. Guo and R. I. Kaiser, *Chemphyschem*, 2008, **9**, 95-105.
20. P. Maksyutenko, F. Zhang, Y. S. Kim, R. I. Kaiser, S. H. Chen, C. C. Wu and A. H. H. Chang, *J. Phys. Chem. A*, 2010, **114**, 10936-10943.
21. D. Sillars, R. Kaiser, N. Galland and Y. Hannachi, *J. Phys. Chem. A*, 2003, **107**, 5149-5156.
22. N. Balucani, F. Zhang and R. I. Kaiser, *Chem. Rev.*, 2010, **110**, 5107-5127.
23. S. Bauer, *Chem. Rev.*, 1996, **96**, 1907-1916.
24. H. F. Bettinger, *Organometallics*, 2007, **26**, 6263-6267.
25. D. S. N. Parker, F. T. Zhang, P. Maksyutenko, R. I. Kaiser and A. H. H. Chang, *Phys. Chem. Chem. Phys.*, 2011, **13**, 8560-8570.
26. D. S. N. Parker, F. T. Zhang, P. Maksyutenko, R. I. Kaiser, S. H. Chen and A. H. H. Chang, *Phys. Chem. Chem. Phys.*, 2012, **14**, 11099-11106.
27. S. Maity, D. S. Parker, B. B. Dangi, R. I. Kaiser, S. Fau, A. Perera and R. J. Bartlett, *J. Phys. Chem. A*, 2013.
28. D. S. N. Parker, N. Balucani, D. Stranges, R. I. Kaiser and A. Mebel, *J. Phys. Chem. A*, 2013, **117**, 8189-8198.
29. R. I. Kaiser, S. Maity, B. B. Dangi, Y.-S. Su, B. J. Sun and A. H. H. Chang, *Phys. Chem. Chem. Phys.*, 2014, **16**, 989-997.
30. D. S. Parker, B. B. Dangi, N. Balucani, D. Stranges, A. M. Mebel and R. I. Kaiser, *J. Org. Chem.*, 2013, **78**, 11896-11900.

31. P. J. Bruna and F. Grein, *J. Phys. Chem. A*, 2001, **105**, 3328-3339.
32. X. Z. Yang and J. E. Boggs, *Chem. Phys. Lett.*, 2005, **410**, 269-274.
33. K.-P. Huber and G. Herzberg, *Constants of Diatomic Molecules*, Van Nostrand Reinhold: New York City, New York, 1979.
34. P. A. Denis, *J. Phys. Chem. A*, 2004, **108**, 11092-11100.
35. R. Kirk and P. Timms, *Chem. Commun. (London)*, 1967, 18-19.
36. R. J. Suffolk, T. A. Cooper, E. Pantelides, J. D. Watts and H. W. Kroto, *J. Chem. Soc., Dalton Trans.*, 1988, 2041-2045.
37. L. Ennis and A. Hitchcock, *J. Chem. Phys.*, 1999, **111**, 3468-3478.
38. C. Kirby, H. W. Kroto and M. J. Taylor, *J. Chem. Soc., Chem. Commun.*, 1978, 19-20.
39. L. Bizzocchi and C. D. Esposti, *J. Mol. Spectrosc.*, 2007, **241**, 67-74.
40. P. Turner and I. Mills, *Mol. Phys.*, 1982, **46**, 161-170.
41. M. T. Nguyen, L. Vanquickenborne, M. Sana and G. Leroy, *J. Phys. Chem.*, 1993, **97**, 5224-5227.
42. R. I. Kaiser, P. Maksyutenko, C. Ennis, F. T. Zhang, X. B. Gu, S. P. Krishtal, A. M. Mebel, O. Kostko and M. Ahmed, *Faraday Discuss.*, 2010, **147**, 429-478.
43. D. S. N. Parker, F. T. Zhang, P. Maksyutenko, R. I. Kaiser and A. H. H. Chang, *Phys. Chem. Chem. Phys.*, 2011, **13**, 8560-8570.
44. X. B. Gu, Y. Guo, F. T. Zhang, A. M. Mebel and R. I. Kaiser, *Faraday Discuss.*, 2006, **133**, 245-275.
45. X. B. Gu, Y. Guo, E. Kawamura and R. I. Kaiser, *J. Vac. Sci. Technol., A*, 2006, **24**, 505-511.
46. J. D. Bittner. Ph. D. thesis, Massachusetts Institute of Technology, Cambridge, MA 02139, U.S.A, 1981.
47. P. S. Weiss. Ph. D. thesis, University of California at Berkeley, Berkeley, California 94720, U.S.A, 1986.
48. R. I. Kaiser, T. N. Le, T. L. Nguyen, A. M. Mebel, N. Balucani, Y. T. Lee, F. Stahl, P. V. Schleyer and H. F. Schaefer, *Faraday Discuss.*, 2001, **119**, 51-66.
49. R. I. Kaiser, D. S. N. Parker, F. Zhang, A. Landera, V. V. Kislov and A. M. Mebel, *J. Phys. Chem. A*, 2012, **116**, 4248-4258.
50. A. D. Becke, *J. Chem. Phys.*, 1993, **98**, 5648-5652.
51. C. T. Lee, W. T. Yang and R. G. Parr, *Phys. Rev. B*, 1988, **37**, 785-789.
52. C. Hampel, K. A. Peterson and H. J. Werner, *Chem. Phys. Lett.*, 1992, **190**, 1-12.
53. G. D. Purvis and R. J. Bartlett, *J. Chem. Phys.*, 1982, **76**, 1910-1918.
54. P. J. Knowles, C. Hampel and H. J. Werner, *J. Chem. Phys.*, 1993, **99**, 5219-5227.
55. M. J. O. Deegan and P. J. Knowles, *Chem. Phys. Lett.*, 1994, **227**, 321-326.
56. M. J. Frisch, G. W. Trucks, H. B. Schlegel, G. E. Scuseria, M. A. Robb, J. R. Cheeseman, J. A. Montgomery, T. Vreven, K. N. Kudin, J. C. Burant, et al. Gaussian 03, revision C. 02, 2008.
57. J. I. Steinfeld, J. S. Francisco and W. L. Hase, *Chemical Kinetics and Dynamics*, Prentice Hall: New Jersey, 1999.
58. R. D. Levine, *Molecular Reaction Dynamics*, Cambridge University Press: Cambridge, UK, 2005.
59. K. H. Kim, S. A. Jahan, E. Kabir and R. J. C. Brown, *Environ. Int.*, 2013, **60**, 71-80.
60. S. A. S. W. B. Miller, D. Herschbach, *Faraday Discuss.*, 1967, **44**, 108-122.
61. N. Balucani, O. Asvany, A. H. H. Chang, S. H. Lin, Y. T. Lee, R. I. Kaiser and Y. Osamura, *J. Chem. Phys.*, 2000, **113**, 8643-8655.
62. C. H. Chin, A. M. Mebel and D. Y. Hwang, *J. Phys. Chem. A*, 2004, **108**, 473-483.

Figures Captions

Figure 1. Products formed in bimolecular gas phase reactions of boron with unsaturated hydrocarbons under single collision conditions in a crossed molecular beams machine.

Figure 2. Products formed in bimolecular gas phase reactions of boron monoxide with unsaturated hydrocarbons under single collision conditions in a crossed molecular beams machine.

Figure 3. Selected time-of-flight (TOF) spectra at mass-to-charge (*m/z*) ratio of 70 ($C_2H_3{}^{11}B^{32}S^+$) (top), and the corresponding laboratory angular distribution (bottom) for the reaction of boron monosulfide ($^{11}B^{32}S$; $X^2\Sigma^+$) with ethylene (C_2H_4; X^1A_g). The circles represent the experimental data points, while the solid lines represent the best fits.

Figure 4. Center-of-mass translational energy flux distribution ($P(E_T)$, top) and center-of-mass angular flux distributions ($T(\theta)$, bottom) for the formation of the $C_2H_3{}^{11}B^{32}S$ product(s) in the reaction of boron monosulfide ($^{11}B^{32}S$; $X^2\Sigma^+$) with ethylene (C_2H_4; X^1A_g). The hatched areas account for the experimental error limits.

Figure 5. The computed $C_2H_4{}^{11}B^{32}S$ potential energy surface (PES) with the relative energies given in kJ mol^{-1}.

Figure 6. Transition state geometries of hydrogen loss steps to product **p1** via the **i1-p1** (left) and **i2-p1**(right) pathways. Bond angles are given in degrees with respect to the molecular rotation plane and the dotted lines represent the distances of the cleavage C-H bond in angstroms.

Figure 7. Predicted products to be formed in the system of boron monosulfide with unsaturated hydrocarbons in a bimolecular gas phase reaction under single collision conditions.

TOC Graph

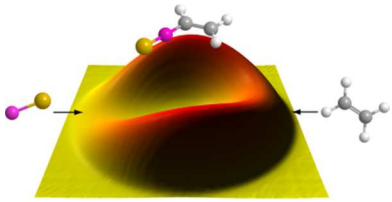

Bimolecular gas phase formation of vinylsulfidoboron ($C_2H_3{}^{11}B^{32}S$) under single collision conditions.

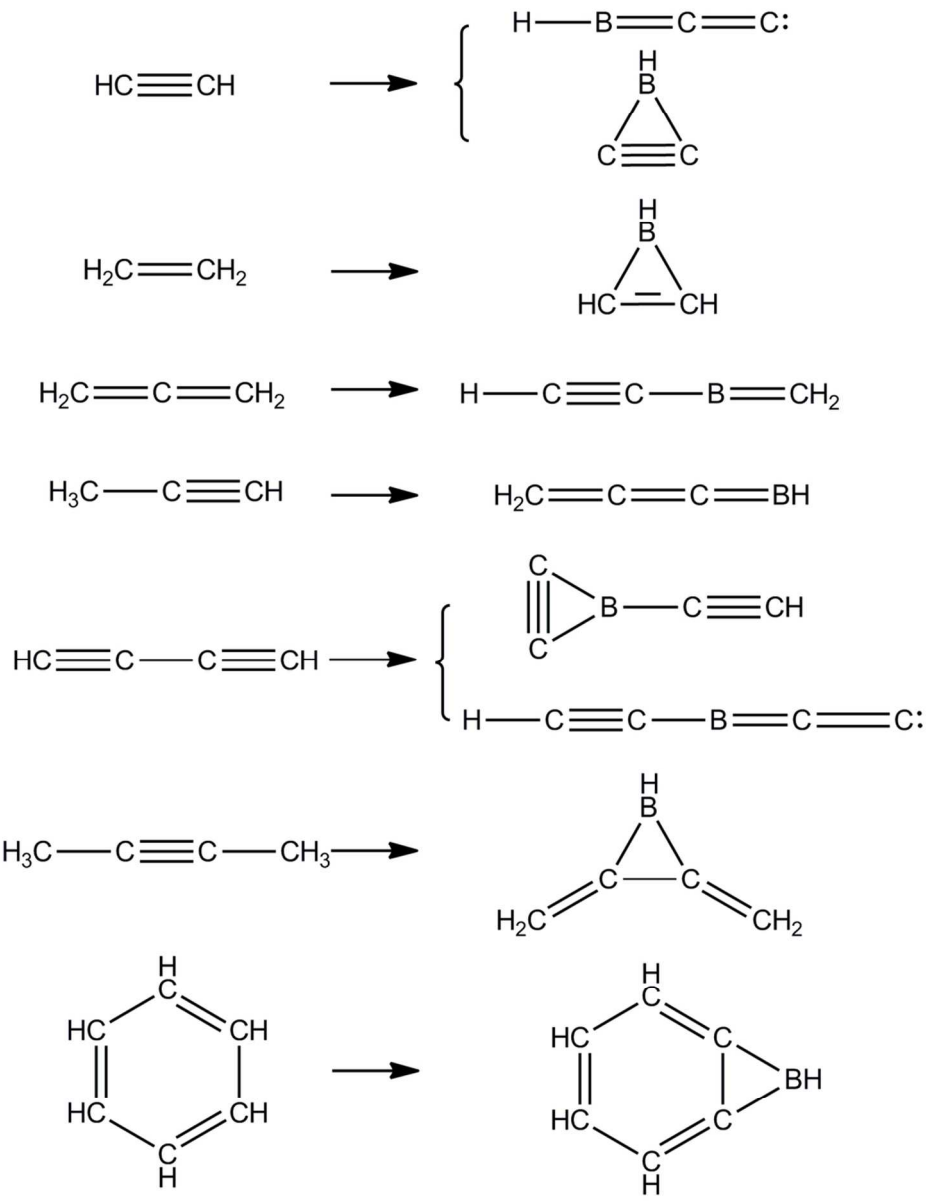

92x118mm (300 x 300 DPI)

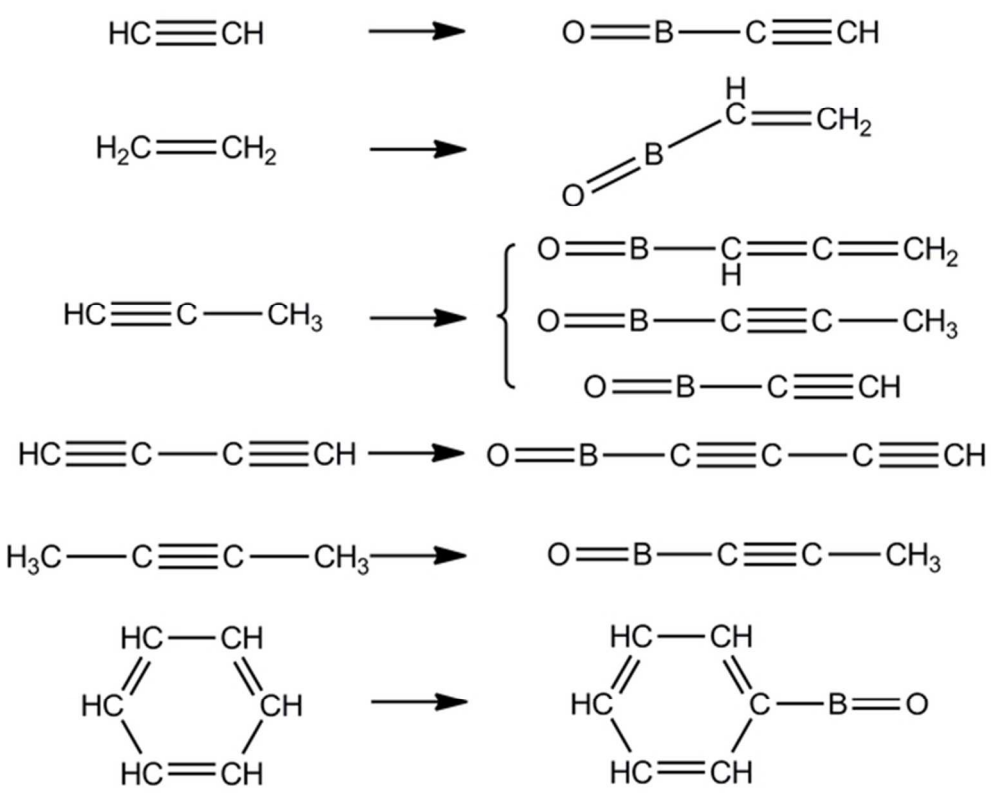

54x43mm (300 x 300 DPI)

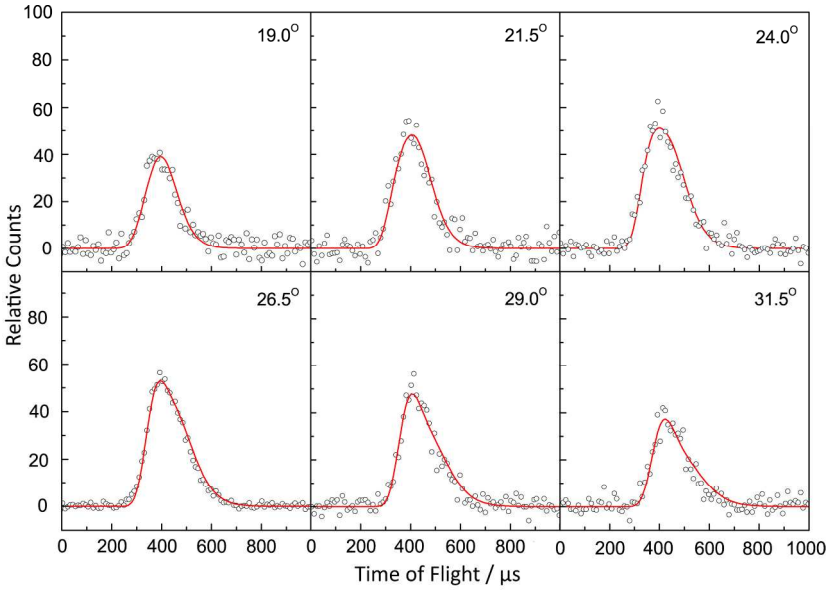

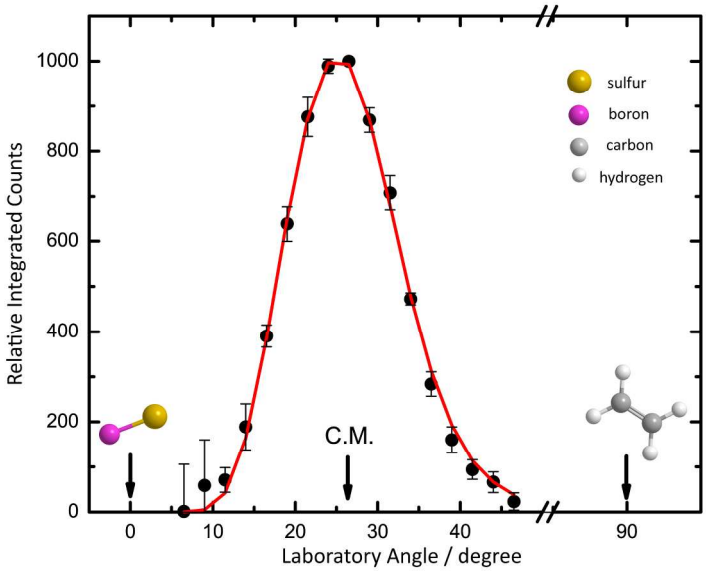

166x241mm (300 x 300 DPI)

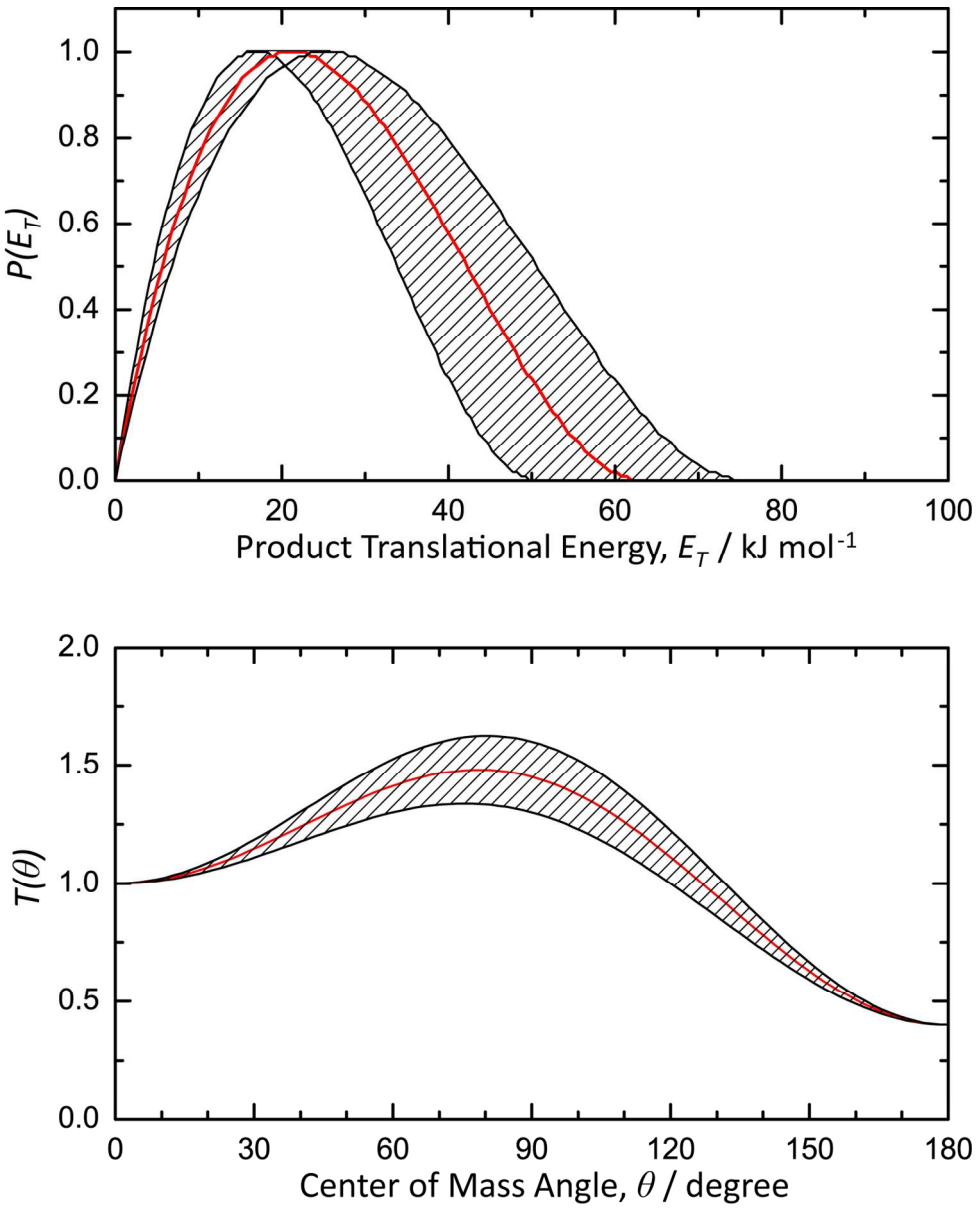

267x330mm (150 x 150 DPI)

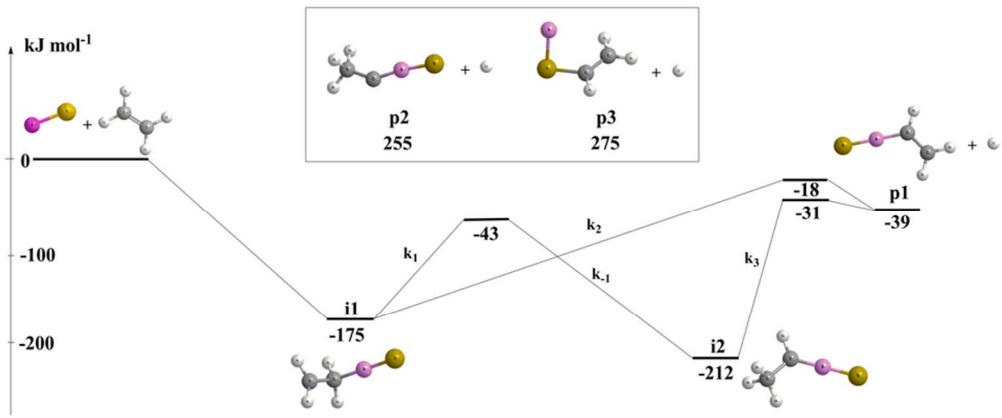

81x33mm (300 x 300 DPI)

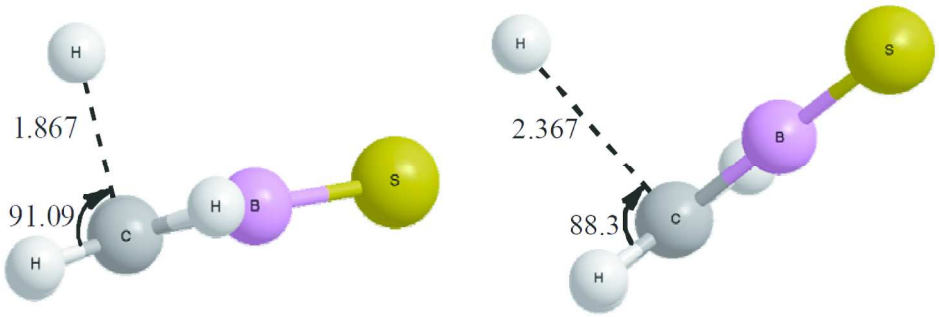

242x80mm (300 x 300 DPI)

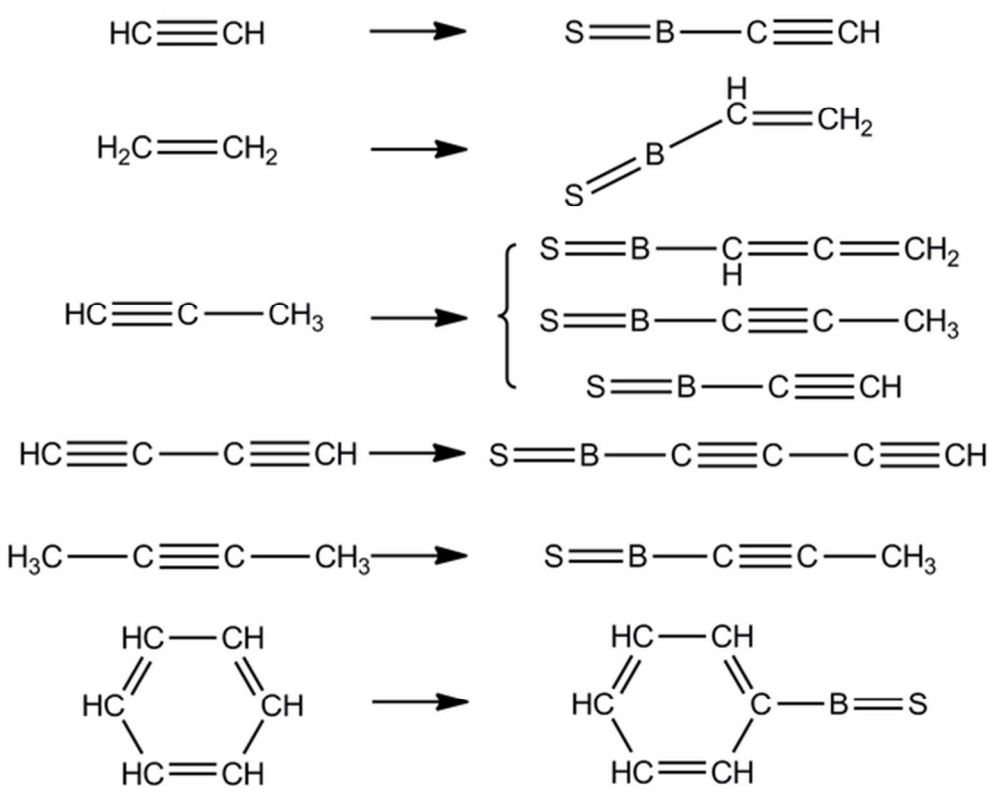

54x43mm (300 x 300 DPI)